Published for SISSA by Springer
Received: August 25, 2011
Revised: November 8, 2011
Accepted: November 9, 2011
Published: November 28, 2011

Downward-going tau neutrinos as a new prospect of detecting dark matter

N. Fornengo and V. Niro

Dipartimento di Fisica Teorica, Università di Torino and INFN, Sezione di Torino, via P. Giuria 1, I-10125 Torino, Italy

E-mail: fornengo@to.infn.it, niro@to.infn.it

Abstract: Dark matter trapped in the Sun produces a flux of all flavors of neutrinos, which then reach the Earth after propagating out of the Sun and oscillating from the production point to the detector. The typical signal which is looked at refers to the muon neutrino component and consists of a flux of up-going muons in a neutrino detector, the major source of background being atmospheric neutrinos. We propose instead a novel signature, namely the possibility of looking at the tau neutrino component of the dark matter signal, which is almost background-free in the downward-going direction, since the tau neutrino amount in atmospheric neutrinos is negligible and in the down-going baseline atmospheric muon-neutrinos have no time to sizably oscillate. We analyze the prospects of studying the downward-going tau neutrinos from dark matter annihilation (or decay) in the Sun in Cherenkov detectors, by looking at hadronic showers produced in the charged-current tau neutrino interactions and subsequent tau decay. We discuss the various sources of background (namely the small tau neutrino component in atmospheric neutrinos, both from direct production and from oscillations; tau neutrinos from solar corona interactions; the galactic tau neutrino component) as well as sources of background due to misidentification of electron and muon events. We find that the downward-going tau neutrinos signal has potentially very good prospects for Mton scale Cherenkov detectors, the main limitation being the level of misidentification of non-tau events, which need to be kept at level of percent. Several tens of events per year (depending on the dark matter mass and annihilation/decay channel) are potentially collectible with a Mton scale detector, and a $5\,\sigma$ significance discovery is potentially reachable for dark matter masses in the range from 20 to 300 GeV with a few years of exposure on a Mton detector.

Keywords: Beyond Standard Model, Cosmology of Theories beyond the SM, Neutrino Physics, Solar and Atmospheric Neutrinos

ArXiv ePrint: 1108.2630

doi:10.1007/JHEP11(2011)133

JHEP11(2011)133

Contents

1 Introduction

It is well established by means of astrophysical and cosmological probes that almost 23% of the matter present in the Universe is in the form of a non-luminous component, the so-called Dark Matter (DM). Although the evidence for DM in cosmic structures is of gravitational origin, it is expected that DM particles may produce a large variety of direct or indirect signals, which represent the subject of a large number of experimental and theoretical studies. While direct searches exploit the direct scattering of DM particles on the nuclei of a low-background detector, indirect signals look for the products of DM self-annihilation (or decay) occurring in the galactic halo, in the extragalactic environment or in those celestial bodies, like the Sun and the Earth, where they can be gravitationally trapped and accumulated before starting the annihilation (or decay) process. All annihilation (or decay) products are absorbed by the bodies, except neutrinos: a flux of high-energy neutrinos, in general composed by all three flavours, can then emerge from the Sun or from the core of the Earth as a signal of the presence of the trapped DM.

The typical way of looking for a signal from DM annihilation in the Sun or in the Earth is to search for an excess of upward-going muons produced by charged current interactions of the ν_μ flux produced by DM annihilation. The advantage to look at the upward-going neutrino flux though its muon conversion is represented by the large conversion area offered by the rock below the detector, and by the well-established and efficient experimental techniques to detect high energy muons. The main source of background is therefore represented by the ν_μ-component of atmospheric neutrinos.

JHEP11(2011)133

A great deal of work has been devoted to these studies, see for instance refs. [1–5], and refs. [6–9] for applications to the case of neutralino DM. Limits on the flux of through-going muons from DM annihilation inside the Sun, the Earth and at the Galactic Center have been set using data from water Cherenkov detectors like Super-Kamiokande (SK) [10] and from neutrino telescopes like AMANDA and IceCube [11, 12]. Competitive limits can also be obtained considering the stopping muons, which are usually the dominant signal for low-mass DM particles. This analysis has been carried out in the context of a light-neutralino signal at SK in ref. [13] and in a more general framework in ref. [14], where fully contained events were also considered. Recently, it has been discussed in ref. [15] the ability of studying the low mass DM range using track events in the DeepCore array of the IceCube detector, that can reach an energy threshold as low as 10 GeV. Detectors designed for other physics searches, such as liquid argon and magnetized iron calorimeter detectors, are able to achieve a much better energy and directional resolution than water Cherenkov detectors and thus could be used for detecting neutrinos from DM annihilations inside the Sun [16, 17]. Moreover, the possibility of detecting DM through electron neutrinos in liquid scintillation experiments like KamLAND has also been considered, see e.g. ref. [18].

In this paper we instead intend to propose and study the feasibility of a different signature: downward-going tau neutrinos produced by DM annihilation in the Sun. The basic motivation is the following: while DM annihilation typically produces similar amounts of all neutrino flavors, atmospheric neutrinos are largely dominated by the ν_e and ν_μ components, the ν_τ's being very suppressed. Neutrino oscillations transform a fraction of the original atmospheric ν_μ into ν_τ, but this phenomenon is basically inoperative in the down-going direction, due to the much larger oscillation length (of the order of the Earth diameter) as compared to the average production height of atmospheric neutrinos, that for definiteness we fixed to be 15 km in the vertical direction (see e.g. ref. [19] for a more precise discussion of the production height). This fact implies that in the downward direction the ν_τ produced inside the Sun by DM annihilation (or decay) represents an almost background-free signal.

We wish to recall that the ν_τ component in the DM neutrino signal coming from the Sun is basically unavoidable: i) the mechanism of production of DM annihilation is hardly flavor-sensitive to the level of producing only ν_e and ν_μ; ii) neutrino oscillations on the baseline of the Sun-Earth distance in any case average out any production of ν_μ into a fraction of ν_τ able to reach the Earth. This implies that the amount of the DM-signal ν_τ's reaching the Earth from the Sun are of the same order of magnitude as the DM-signal ν_μ's, but they are basically background-free. Therefore they may be a competitive discovery channel as compared to the standard up-going ν_μ's signal, which is affected by a much larger background represented by atmospheric ν_μ's.

The background sources for the ν_τ channel are represented by the very small intrinsic ν_τ production from cosmic-rays interactions in the atmosphere (atmospheric ν_τ's) or by residual atmospheric ν_μ oscillation, negligible for down-going but more relevant for almost horizontal fluxes, by oscillation of ν_e and ν_μ produced by cosmic-rays interactions in the solar corona (which represent an irreducible background for our DM signal, since it comes from the same source, the Sun) and by a galactic plane ν_τ flux, mainly given

JHEP11(2011)133

by oscillation of ν_μ produced in cosmic-ray interactions with the interstellar medium (this source of background is, in principle, reducible by angular cuts on the galactic plane position). We will show that these sources of backgrounds are, by themselves, not posing significant limits to the DM signal, which therefore represents a potentially viable novel possibility.

We will instead show that the limiting factor for an analysis of the downward-going ν_τ's is the ability of a neutrino detector to identify the tau neutrinos. We will concentrate on water Cherenkov detectors, in order to be able to access the relatively low energies which are relevant for DM studies ($E_\nu <$ TeV) (in the case of DM with mass from few tens of GeV to few TeV). Since next generation apparata of Mton scale are currently under study, our predictions are particularly suited for future water Cherenkov detectors like the Hyper-Kamiokande (HK) project [20].

A signal from tau neutrinos, specifically in connection with DM searches, have been also studied in ref. [21], where the possibility to detect ν_τ from gravitino DM decay in the halo of our Galaxy was discussed. High energetic neutrinos ($E_\nu \geq$ TeV) coming from astrophysical sources have been considered in refs. [22, 23], where the flux of ν_τ arising from neutrino oscillation was discussed. The ability to detect atmospheric tau neutrino events through an ultra-large liquid argon detector is described in ref. [24]. An experimental measurement to detect tau atmospheric neutrinos by measuring the energy spectra of neutrino induced showers has been suggested in ref. [25].

The scheme of the present paper is the following. In section 2 we will discuss the neutrino fluxes coming from DM annihilation and the background fluxes: the atmospheric, solar corona and galactic neutrinos. The class of signals relevant to water Cherenkov detectors and a discussion about the experimental limits in detecting ν_τ in those type of detectors is given in section 3. The calculation of the hadronic contained events is then presented in section 4, both for the signal and for the various sources of background. The capabilities of Mton-scale water Cherenkov detectors on the discovery of the ν_τ signal from DM annihilation coming from the Sun is derived in section 5, where we discuss also the level of sensitivity that can be achieved from this detection channel on the DM-proton scattering cross section σ_p. Conclusions are given in section 6.

2 Neutrino fluxes

Let us start by discussing the relevant neutrino fluxes produced by DM annihilation in the Sun. The decay case is easily obtained along the same line of reasoning. We are interested not only on the source spectra, but also in the propagated fluxes which reach the Earth, and that go through both energy redistribution inside the solar medium and oscillation processes. We will discuss and treat all these phenomena as in ref. [26].

In addition to the DM signal, we need to discuss the relevant sources of background for the ν_τ signal, which arise from atmospheric, solar corona and galactic cosmic-rays interactions.

JHEP11(2011)133

2.1 Dark matter

The neutrino flux at the detector, coming from DM annihilation inside the Sun and for each of the three neutrino flavours, is defined as:

$$\frac{d\phi_\nu}{dE_\nu} = \sum_f \mathrm{BR}_f \frac{\Gamma_\odot}{4\pi d^2} \frac{dN_\nu^f}{dE_\nu} \tag{2.1}$$

where BR_f is the DM branching ratio into the annihilation final-state channel f, dN_ν^f/dE_ν are the neutrino spectra for each channel f, $\Gamma_\odot$ denotes the annihilation rate inside the Sun and d is the distance between the Earth and the Sun. For definiteness, in our analysis we will consider two specific annihilation channels: i) direct annihilation into neutrinos with flavor-blind branching ratios, i.e., $\mathrm{BR}_{\nu_e\bar{\nu}_e} = \mathrm{BR}_{\nu_\mu\bar{\nu}_\mu} = \mathrm{BR}_{\nu_\tau\bar{\nu}_\tau} = 1/3$; ii) annihilation into $\tau\bar{\tau}$ leptons with $\mathrm{BR}_{\tau\bar{\tau}} = 1$. More general situations are easily implemented. The DM fluxes dN_ν^f/dE_ν are calculated as described in refs. [26, 27], considering all physical processes that can occur to the neutrinos from the production point inside the Sun to the detector at the Earth: vacuum and matter neutrino oscillations, neutral current and charged current interactions on the Sun's medium. We have fixed the neutrino mixing angles as [28]: $\sin^2\theta_{23} = 0.5$, $\sin^2\theta_{12} = 0.304$ and $\theta_{13} = 0$. The annihilation rate $\Gamma_\odot$ is calculated as in ref. [29–31]. For the DM velocity distribution in the rest frame of the Galaxy we have assumed a Maxwellian distribution with $\bar{v} = 220\,\mathrm{km\,s^{-1}}$ and we have fixed the local DM density ρ_0 to be $0.3\,\mathrm{GeV\,cm^{-3}}$. The annihilation rate depends on the DM-proton scattering cross section, which we will fix to benchmark values in our analysis, as specified in the following.

Since we are interested in the (downward going) neutrino flux coming from the Sun, it can be important to know the amount of time spent by the Sun at different zenith angles above the horizon. This is relevant to determine the duty factor of the signal and could also be exploited for optimizing the signal-to-background ratio, in the case the detection of the ν_τ flux could be correlated to the Sun's position in the sky. If we consider a detector located at a latitude φ, then the motion of the Sun is described by the following expression [32]:

$$\cos\theta_Z = \sin\varphi\,\sin\delta + \cos\varphi\,\cos\delta\,\cos\theta_{\mathrm{HA}} \tag{2.2}$$

where θ_Z is the zenith angle, δ is the solar declination and θ_{HA} is the hour angle. The value of δ can be obtained using an approximate expression,

$$\delta = 23.45^\circ \sin\left(\frac{360^\circ(N_{\mathrm{day}} - 80)}{365}\right), \tag{2.3}$$

where N_{day} denotes the number of the day, starting on the first of January. The hour angle θ_{HA} is zero at the local solar noon and indicates the time that has passed since the Sun was at the local meridian. In the left panel of figure 1 we report the apparent motion of the Sun, considering a detector located at a latitude $\varphi = 36^\circ$, that is roughly the latitude of the Kamioka site. In the right panel of figure 1 the amount of time (in hours) spent in one year by the Sun in each zenith-angle bin is shown, for the same latitude: this determines the yearly duty-factor for the signal. Since ν_τ's produced in the galactic plane are one of

JHEP11(2011)133

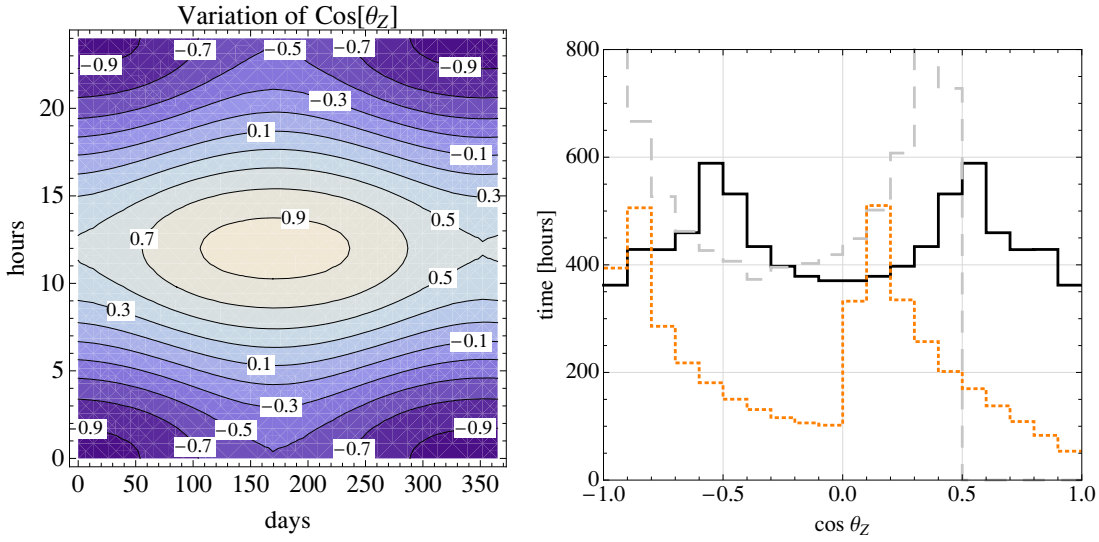

Figure 1. *Left panel*: apparent motion of the Sun as a function of time (hour and day of the year), for a detector located at the latitude $\varphi = 36°$. The regions denoted by different shades denote the value of the cosine of the zenith angle (shown by the numbers in labels) occupied by the Sun at a given day and hour. Positive values of $\cos\theta_Z$ refers to the Sun above the horizon. *Right panel*: amount of time (in hours) spent by the Sun in each zenith-angle bin in one year, for a latitude $\varphi = 36°$ (solid line). The dashed gray line shows the time spent by the galactic center in each zenith-angle bin. The dotted orange line represents the averaged duty factor of the galactic plane convoluted with the position of the Sun, see text for more details.

our sources of background, in the same right panel of figure 1 we also show the time that the galactic plane spends in each zenith angle bin. We have averaged over 120 points in the galactic plane ($b = 0$) and for each bin above (below) the horizon we have imposed the condition that also the Sun position is above (below) the horizon, even if not in the same angular bin of the galactic plane. This is done to determine the duty-factor of the galactic-plane contribution correlated with the presence of the Sun in the upper (or lower) hemisphere. For this reason, the integral of the galactic plane duty-factor over the total zenith angle bins does not turn out to be one year. Just for definiteness, we also show in figure 1 the duty-factor of the galactic center without considering the position of the Sun. In this case the duty-factor is zero for $\cos\theta_Z > 0.5$.

2.2 Backgrounds

There are various sources of background for the ν_τ signal from DM annihilation. First of all we have the ν_τ atmospheric background coming from oscillation of atmospheric ν_μ. This form of background is the dominant one for upward-going neutrinos, but it is extremely reduced for the downward-going case that we are going to consider. For the atmospheric neutrino, we have used the Honda fluxes [33], considering the new release from February 2011, where the implementation of the JAM interaction model [34] for the low energy interactions of cosmic rays and air nuclei was implemented. We considered the azimuth-angle-averaged flux at Kamioka site with mountain over the detector.

JHEP11(2011)133

A second form of background is given by the intrinsic ν_τ contribution to the atmospheric flux coming from decay of charmed particles. This has been computed in ref. [35] and can be described by the following parameterization:

$$\log_{10}\left[E_\nu^3 \frac{d\phi_\nu}{dE_\nu} / \left(\frac{\mathrm{GeV}^2}{\mathrm{cm}^2\,\mathrm{s}\,\mathrm{sr}}\right)\right] = -A + Bx - Cx^2 - Dx^3, \tag{2.4}$$

which is valid for $10^2\,\mathrm{GeV} \leq E_\nu \leq 10^6\,\mathrm{GeV}$, with $x = \log_{10}(E_\nu[\mathrm{GeV}])$, $A = 6.69$, $B = 1.05$, $C = 0.150$ and $D = -0.00820$. We have extrapolated the flux down to $E_\nu^{\mathrm{min}} = 3.5\,\mathrm{GeV}$, that is the minimal neutrino energy required for the production of a tau lepton. In order to check our extrapolation, we have compared the fluxes that we obtain in this way with the ones reported in ref. [36]. We found that for energies $E_\nu \leq 10\,\mathrm{GeV}$ our results are in well agreement with [36], since the ν_τ fluxes are dominated by the oscillated atmospheric neutrinos in that range of energies. For $10\,\mathrm{GeV} < E_\nu \leq 10^2\,\mathrm{GeV}$, our results are equivalent to [36] for the horizontal direction, while they differ by at most a factor of two for the down-going direction ($\cos\theta_z = 1$). We have checked, however, that the events coming from this energy range account for roughly the 11% of the total ν_τ events, that we will present in section 3. In the same section, we will see that the actual experimental background is highly dominated by the misidentified events. Thus, we expect that our extrapolation of the intrinsic fluxes between 10 and $10^2\,\mathrm{GeV}$ does not have a relevant impact on our analysis (we will comment more precisely on this in section 5). We want, moreover, to stress that the calculation of the intrinsic ν_τ component for energies $E_\nu > 10^2\,\mathrm{GeV}$ suffers from sizable uncertainties. In fact, the atmospheric showering parameters are not precisely known [37] and in the literature different charm production models are present: quark gluon string model [38], recombination quark proton model [39] and perturbative QCD [40]. The fluxes that we use in this article are based on a perturbative QCD approach [35], but depending on the specific models, the predictions for the fluxes might change of up to one orders of magnitude. We refer to refs. [37, 41–43] for a detailed discussion on this topic and we will comment in section 5 on possible implication of this uncertainties on DM searches. In the following, when we refer to 'atmospheric' ν_τ flux we will always imply the sum of the oscillated fluxes from atmospheric ν_μ and the intrinsic contribution.

The third form of background is represented by the neutrino flux produced in the solar corona by cosmic-ray collisions. This has been studied in ref. [44], where a suitable parameterization of the flux of electron and muon neutrinos ($j = \nu_e, \nu_\mu$) has been determined:

$$\frac{d\phi_j}{dE_\nu} = N_0 \frac{(E_\nu[\mathrm{GeV}])^{-\gamma-1}}{1 + A(E_\nu[\mathrm{GeV}])}\,(\mathrm{GeV}\,\mathrm{cm}^2\,\mathrm{s})^{-1}, \tag{2.5}$$

which is valid for $10^2\,\mathrm{GeV} \leq E_\nu \leq 10^6\,\mathrm{GeV}$. For the numerical values of the coefficients N_0, A and γ we refer to ref. [44]. Also in this case we have extrapolated the neutrino fluxes down to $E_\nu^{\mathrm{min}} = 3.5\,\mathrm{GeV}$. During their propagation to the Earth, the electron and muon neutrinos produced in the solar corona oscillate and generate ν_τ.

Finally, the fourth possible source of background is given by the fluxes of tau neutrinos from the Galactic plane. A complete discussion of this topic is presented in ref. [45, 46].

JHEP11(2011)133

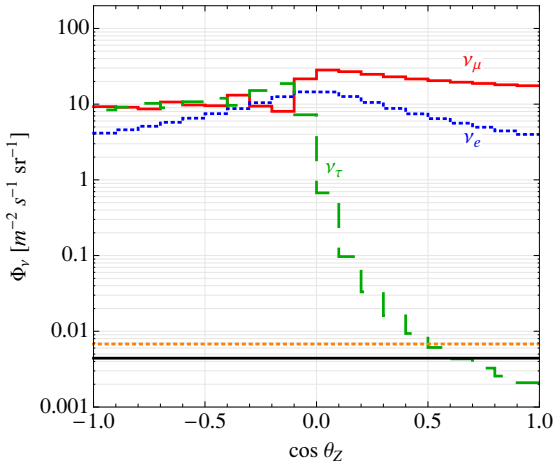

Figure 2. Atmospheric neutrino fluxes as a function of the zenith angle $\cos\theta_Z$ at Kamioka site. The dotted (blue), solid (red) and dashed (green) line refer to the ν_e, ν_μ and ν_τ fluxes at the detector (with oscillation included). The solid horizontal (black) line denotes the ν_τ flux from solar corona interaction, while the dotted horizontal (orange) line refers to the level of the galactic ν_τ flux. Note that these two fluxes (differently from the atmospheric contributions) are present only when the Sun or the galactic plane occupy each specific angular bin. Fluxes have been integrated from $E_\nu^{\rm min} = 3.5\,{\rm GeV}$.

The ν_τ flux can be parameterized as:

$$\frac{d\phi_\nu}{dE_\nu} = 9\times 10^{-6}\,({\rm GeV\,cm^2\,s\,sr})^{-1}(E_\nu[{\rm GeV}])^{-2.64}, \tag{2.6}$$

which is valid in the energy range $1\,{\rm GeV} \leq E_\nu \leq 10^3\,{\rm GeV}$. As discussed in connection with figure 1, for a detector located at a latitude $\varphi = 36^\circ$ this contribution starts to be sizable for $\cos\theta_Z \lesssim 0.5$. In this range of zenith angles the atmospheric and intrinsic fluxes are by far the dominant ones and thus, for the ν_τ signal coming from the Sun, the galactic neutrinos do not represent a troublesome source of background. We have nevertheless included this contribution in the calculation.

Figure 2 shows the total neutrino fluxes (integrated from $E_\nu^{\rm min} = 3.5\,{\rm GeV}$ up to $E_\nu^{\rm min} = 10^4\,{\rm GeV}$) as a function of the zenith angle $\cos\theta_Z$. It is well visible how the atmospheric ν_τ background is sizebly reduced for $\cos\theta_Z \geq 0$ as compared to the $\cos\theta_Z \leq 0$ case and how the ν_τ flux is much smaller than the ν_e and ν_μ fluxes. This behavior is the main motivation for our proposal on downward-going tau events. In fact, as already discussed above, the DM ν_τ signal from the Sun is comparable, in size, with the ν_μ signal. Nevertheless, the up-going muon channel (measured through up-going muons) has a much larger atmospheric background than the down-going tau channel, as is clearly seen in figure 2. An up-going muon signal which occurs to be completely dominated by the atmospheric neutrino background, could instead dominate the atmospheric background in the down-going tau channel. In figure 2 we also show the solar corona and the galactic ν_τ fluxes. We notice that solar corona neutrinos become non-negligible mainly for $\cos\theta_Z \gtrsim 0.5$, while the galactic neutrinos are more important for angles with $\cos\theta_Z < 0.5$. For the down-

JHEP11(2011)133

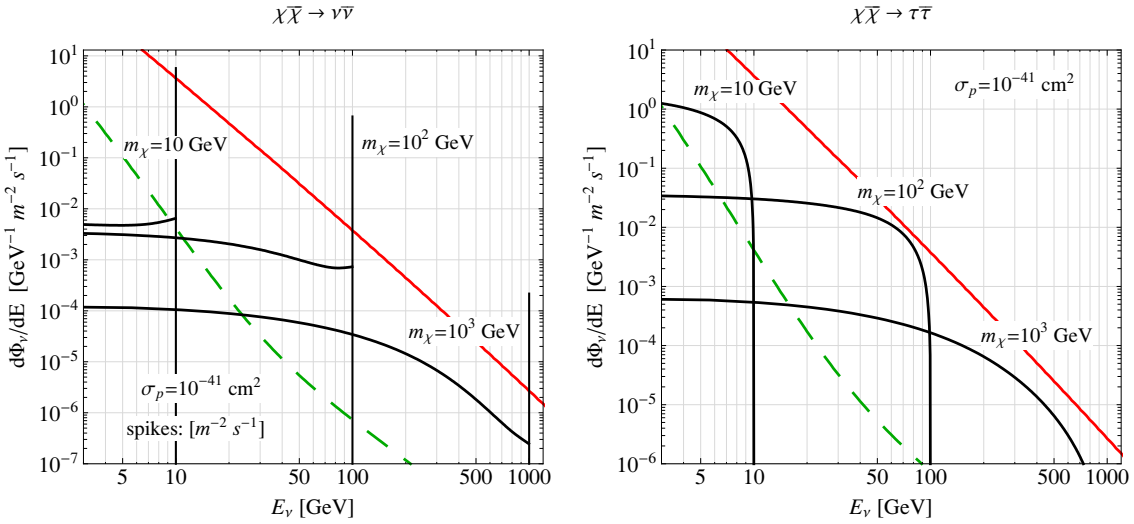

Figure 3. Fluxes of ν_τ arising from DM annihilation inside the Sun: the left panel refers to the case of direct annihilation into neutrinos with even branching ratios in the three flavours, while the right panel stands for annihilation into tau leptons. In the left panel, the continuum part of the spectrum is in units of $\mathrm{GeV}^{-1}\,\mathrm{m}^{-2}\,\mathrm{s}^{-1}$, while the line is in units of $\mathrm{m}^{-2}\,\mathrm{s}^{-1}$. The DM spin-independent scattering cross section σ_p is fixed at the value $10^{-41}\,\mathrm{cm}^2$ and the cases for DM masses of 10, 100 and 1000 GeV are reported. The solid (red) line shows the downward-going flux of atmospheric *muon* neutrinos ν_μ, while the long-dashed (green) line refers to the downward-going background flux of ν_τ (sum of atmospheric, both intrinsic and from oscillation, solar corona and galactic fluxes). The fluxes have been integrated over zenith angles with $\cos\theta_Z \geq 0$.

going ν_τ signal, atmospheric neutrinos represent the main source of background, while the galactic and solar corona neutrinos give a sizable contribution for small and large zenith angles respectively. In both cases, they are very suppressed, therefore offering potential chances to a signal to emerge.

A few examples of downward-going ν_τ fluxes as a function of the neutrino energy E_ν are shown in figure 3, together with the total downward-going ν_τ background fluxes: sum of atmospheric, both intrinsic and from oscillation, solar corona and galactic fluxes. To allow for a realistic comparison between the fluxes, in summing the galactic and solar contributions to the atmospheric ones, we have multiplied by the fraction of the time that the Sun or galactic plane spend in each zenith angle bin with respect to the total time that the Sun spends above the horizon in one year. We have integrated over zenith angles with $\cos\theta_Z \geq 0$. This represents the angular range that we will consider throughout the paper. For the signal, we show the cases for DM mass of 10, 100, 1000 GeV, and for the DM spin-independent scattering cross section σ_p we have used a benchmark value of $10^{-41}\,\mathrm{cm}^2$ (with σ_p we will denote throughout the paper the spin-independent scattering cross section, while with σ_p^{SD} the spin dependent one). The left and right panels refer to the two benchmark annihilation channels: direct annihilation into neutrinos and annihilation into tau leptons. In the case of direct annihilation into neutrinos, we clearly notice the line a $E_\nu = m_\chi$ together with the degraded-energy tail due to neutrino propagation in the Sun's interior. Also from figure 3 we can see that the signal is significantly dominant over the background

JHEP11(2011)133

in the down-going ν_τ channel, especially at high energies where the tau cross section is not suppressed by mass threshold. In the same figure, we also show the flux of down-going atmospheric ν_μ, which (together with the down-going ν_e) will produce a source of background events for the down-going ν_τ signal in water Cherenkov detectors, due to misidentification of the muon and electron events in the detector, as will be discussed in section 3.

3 Signals at water Cherenkov detectors

The experimental signals of high-energetic tau neutrinos have been analyzed in ref. [47], where the double bang and lollipop signatures were considered. These signatures, however, are distinctive only for energies above the PeV range. For lower energies, between TeV and PeV range, it might be possible to tag taus which decay to muons, if the neutrino interaction vertex occurs within the detector [47].

For the range of energies we are interested in (GeV–TeV), charged-current ν_τ interactions in water Cherenkov detectors will lead to multiple Cherenkov rings and the possibility of individually identifying these events is currently based only on statistical methods. In ref. [48, 49] the SK Collaboration has employed neural network and maximum likelihood techniques to successfully discriminate tau neutrino events. They concentrate on the hadronic decays of tau leptons ($\mathrm{BR}_\tau^h \simeq 64\%$), since they have a more spherical topology than the backgrounds. We will exploit the same type of signature in our calculations. The primary backgrounds to ν_τ charged-current events are neutral-current and charged-current events from ν_e and ν_μ atmospheric neutrinos. A number of event selection criteria [48, 49] can be applied to reduce these backgrounds. Using a likelihood analysis and a neural network, the SK Collaboration achieved an efficiency (with respect to the total number of events in the fiducial volume) of 43.1% and 39.0% for tau events identification, respectively. The electron and muon events are misidentified as tau events with a percentage of 3.8% and 3.4% for the same two statistical analyses. Since the atmospheric ν_e and ν_μ fluxes are usually larger than or of the same order of the DM fluxes, as can be seen in figure 3, the misidentification has a relevant impact on the actual performance of water Cherenkov detectors in identifying ν_τ events.

In our analysis we have focused on the favourable situation in which the track events from ν_μ charged current interactions will always be detected and correctly identified. For this reason, in the misidentified background events we will only considered neutral-current events from ν_e and ν_μ atmospheric neutrinos and charged-current events from ν_e interactions. Note that in principle also ν_e and ν_μ from solar corona interactions will contribute to this form of background, but they are negligible with respect to the atmospheric ν_e and ν_μ. Another possible form of background events is represented by neutral-current events from ν_τ (atmospheric, intrinsic and solar corona contributions) and by ν_τ charged-current interaction, with tau decaying into electron. We will neglect these events since we will numerically see that the background is typically dominated by neutral current ν_e and ν_μ and by charged-current ν_e misidentified events. Finally, we wish to comment that also ν_μ and ν_e fluxes from DM annihilations would contribute to the signal events, again through misidentification. We will not include this type of contribution, which is marginal in determining the amount of signal events.

JHEP11(2011)133

4 Contained hadronic events

The class of signal events we are considering is represented by the charged-current production of a tau lepton, followed by its hadronic decay. The hadronic showers of the decay produce Cherenkov rings in the water detector. In this section we discuss our determination of the number of hadronic events, and the calculation of the class of events which contribute to the background through misidentification, namely background events from ν_e and ν_μ neutral current interactions and from ν_e charged current interactions.

4.1 Signal events from hadronic tau decay

For the calculation of contained tau events, we will use the derivation of ref. [50], where the concept of visible energy is introduced. On this topic, see also refs. [23, 25, 51]. For this category of events, the visible energy $E_{\rm vis}$ is the sum of the energy $E_{h,1}$ of the broken nucleon and the hadronic energy $E_{h,2}$ of the tau decay. The total number of contained events for charged current ν_τ interactions is:

$$N_\tau^{\mathcal{CC}}\big|_{\mathcal{S},\mathcal{B}} = M_{\rm det} N_y \times \int_{E_{\rm vis}^{\rm min}}^{E_{\rm vis}^{\rm max}} dE_{\rm vis} \int d\Omega\ \eta(\theta)\, \frac{d\mathcal{I}_\tau^{\mathcal{CC}}}{d\Omega\, dE_{\rm vis}}\bigg|_{\mathcal{S},\mathcal{B}}, \tag{4.1}$$

where $M_{\rm det}$ is the detector mass, N_y the number of years of exposure and $\eta(\theta)$ is the on-source duty factor. For the signal, we use the duty-factor discussed in section 2.1 and shown in the right panel of figure 1. For the background events we have conservatively considered the case in which the events are classified only as upward/downward. Thus, the background is not filtered through the duty-factor of figure 1, instead it is always present when the Sun is above the horizon ($\eta = 1/2$). In a more optimistic scenario in which the detector would be able to correlate the direction of the observed Cherenkov rings of the hadronic showers with the position of the Sun, a reduction of the background would be possible. We will nevertheless neglect this optimistic possibility here and we will consider only the more conservative case in which the events are identified as upward-going or downward-going.

The function $d\mathcal{I}_\tau^{\mathcal{CC}}/d\Omega\, dE_{\rm vis}$ in eq. (4.1) is defined as:

$$\frac{d\mathcal{I}_\tau^{\mathcal{CC}}}{d\Omega\, dE_{\rm vis}}\bigg|_{\mathcal{S},\mathcal{B}} = \int dE_\nu \int dE_\tau \frac{d\phi_{\nu_\tau}}{d\Omega dE_\nu}\bigg|_{\mathcal{S},\mathcal{B}} \Sigma_\tau^{\mathcal{CC}}(E_\tau, E_\nu)\, \frac{d\Gamma_h}{dE_{\rm vis}} + (\nu \to \bar{\nu})\,, \tag{4.2}$$

where $\mathcal{S}$ and $\mathcal{B}$ denote signal and background, respectively, $d\phi_{\nu_\tau}/d\Omega dE_\nu$ is the ν_τ flux coming from DM annihilation or the background flux of atmospheric, intrinsic and solar corona tau neutrinos. The function $\Sigma_\tau^{\mathcal{CC}}$, defined as:

$$\Sigma_\tau^{\mathcal{CC}}(E_\tau, E_\nu) = N_A \left(\mathcal{Z} \frac{d\sigma_{\nu_\tau}^p}{dE_\tau}(E_\tau, E_\nu) + \mathcal{N} \frac{d\sigma_{\nu_\tau}^n}{dE_\tau}(E_\tau, E_\nu) \right) \tag{4.3}$$

quantifies the number of interactions, with N_A being the Avogadro's number, $\mathcal{Z}$ and $\mathcal{N}$ the fraction of proton and neutrons present in the detector and $d\sigma_{\nu_\tau}^{p,n}/dE_\tau$ the ν_τ charged-current cross section on proton and neutron, for which we adopt ref. [52, 53], where the correction due to the finite tau mass is implemented. For the parton distribution functions (PDF) we have chosen the MSTW 2008 NNLO [54, 55] varying Q^2 from $5\,{\rm GeV}^2$ till

JHEP11(2011)133

$10^4\,\mathrm{GeV}^2$. For lower Q^2 we have frozen the PDF to the values assumed at $Q^2 = 5\,\mathrm{GeV}^2$. For a more refined calculation, it should be taken into account also the non-perturbative [56] evolution of the PDF in the low Q^2 region, $Q^2 \lesssim 2\,\mathrm{GeV}^2$. Moreover, also target mass correction [57] could have some impact for very precise estimates. Nevertheless, we have neglected these two latter corrections, since they are beyond the precision required for our study. We have checked that with our assumption we achieve an agreement better than 10% with the total cross section reported in ref. [52, 53].

The function $d\Gamma_h/dE_{\rm vis}$ in eq. (4.2) is defined as the decay rate of tau leptons into hadrons, provided that the energy of the hadronic decays $E_{h,2}$ is equal to the tau lepton energy minus the final neutrino energy E_{ν_f}, with $E_{\nu_f} = E_\nu - E_{\rm vis}$:

$$\frac{d\Gamma_h}{dE_{\rm vis}} \equiv \int dE_{h,2} \frac{dn_h}{dE_{h,2}}\, \delta\Big(E_{h,2} - \big(E_\tau - (E_\nu - E_{\rm vis})\big)\Big)\, \Theta(E_\nu - E_{\rm vis}) \tag{4.4}$$

The decay rate $dn_h/dE_{h,2}$ can be obtained from the ν_τ spectra produced in the decay:

$$\frac{dn_h}{dE_{h,2}} = \frac{1}{E_\tau}\frac{dn_h}{dz_h} \qquad \text{with} \qquad z_h = \frac{E_{h,2}}{E_\tau}\,, \tag{4.5}$$

where

$$\frac{dn_h}{dz_h} = \frac{dn_\nu}{dz_\nu} \qquad \text{with} \qquad z_\nu = \frac{E_\nu - E_{\rm vis}}{E_\tau}\,. \tag{4.6}$$

The expressions of dn_ν/dz_ν are given in refs. [23, 35, 58]. Note that the function $dn_h/dE_{h,2}$ is normalized to the total branching ratio of tau into hadrons, $\mathrm{BR}_\tau^h = 0.64$.

Using the previous definitions, we can rewrite eq. (4.2) as:

$$\left.\frac{d\mathcal{I}_\tau^{\mathcal{CC}}}{d\Omega\, dE_{\rm vis}}\right|_{\mathcal{S},\mathcal{B}} = \int_{E_{\rm vis}}^{\infty} dE_\nu \int_{E_\tau^{\rm min}}^{E_\nu} dE_\tau \left.\frac{d\phi_{\nu_\tau}}{d\Omega dE_\nu}\right|_{\mathcal{S},\mathcal{B}} \Sigma_\tau^{\mathcal{CC}}(E_\tau, E_\nu)\frac{1}{E_\tau}\frac{dn_\nu}{dz_\nu}\,, \tag{4.7}$$

with an analogous part for antineutrinos and with $E_\tau^{\rm min} = \max[m_\tau, E_\nu - E_{\rm vis}]$. We have considered a lower limit on the visible energy equal to the minimal neutrino energy for tau lepton production: $E_{\rm vis}^{\rm min} = 3.5\,\mathrm{GeV}$. A specific detector should choose the minimal visible energy able to maximize the number of correctly identified tau events with respect to the misidentified ones. This quantity could turn out to be different from our choice of $E_{\rm vis}^{\rm min}$, but this would be highly detector dependent and should be obtained through dedicated Monte Carlo analyses. We fix the upper limit on the visible energy to $E_{\rm vis}^{\rm max} = 10^4\,\mathrm{GeV}$ for the atmospheric events, or to $E_{\rm vis}^{\rm max} = m_\chi$ for the DM events.

The number of signal events expected for a detector of a given exposure (expressed in kton $\times$ year) is shown in figure 4 as a function of the DM mass, for the two cases of DM annihilation into neutrinos (left panel) and annihilation into tau leptons (right panel). The elastic scattering cross section on protons, relevant for capture in the Sun and that determines the size of the annihilation rate $\Gamma_\odot$, is fixed at the benchmark value of $10^{-41}\,\mathrm{cm}^2$. In all our analyses we are considering that equilibrium between capture and annihilation has been reached, as typically occurs for the Sun. The solid (red), dotted (blue) and dashed (black) lines refer to 5, 10 and 50 events in the water Cherenkov detector, respectively. The two horizontal (pink) lines denote the exposures that can be reached by a 0.5 Mton

JHEP11(2011)133

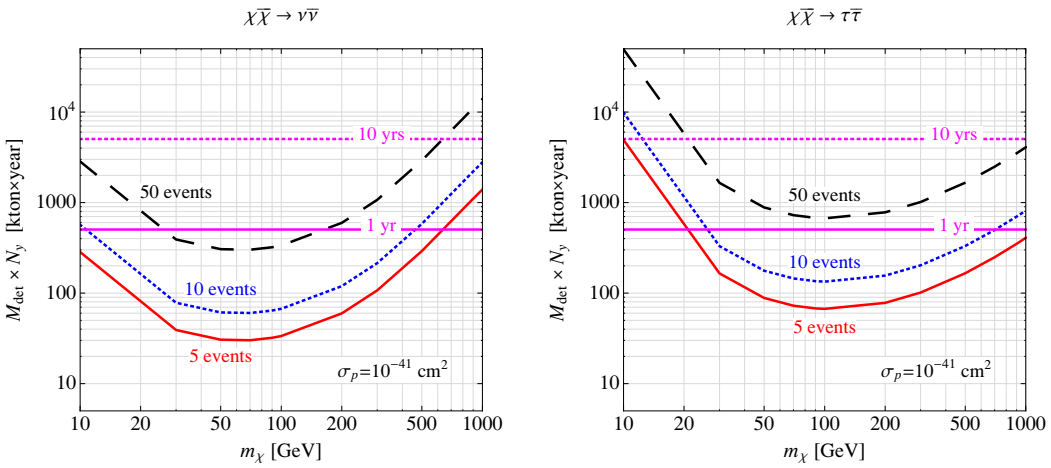

Figure 4. Iso-contours of number of downward-going ν_τ hadronic events in the plane of detector exposure (in kton × year) and DM mass m_χ. The left panel refers to DM annihilation into neutrinos, while the right panels stands for annihilation into tau leptons. The elastic scattering cross section on protons (relevant for capture in the Sun) is fixed at the benchmark value of 10^{-41} cm^2. The solid (red), dotted (blue) and dashed (black) lines refer to 5, 10 and 50 events in the detector, respectively. The two horizontal (pink) lines denote the exposures that can be reached by a 0.5 Mton detector, like HK, in 1 (solid) and 10 (dotted) years.

detector, like HK, in 1 (solid) and 10 (dotted) years. We notice that for a Mton-scale detector, the expected number of down-going ν_τ signal events can reach the level of 50 or more, depending on the DM mass. For a prolonged exposure of a decade or more, more than a hundred of signal events is potentially under reach. For the annihilation channels under study, this signal is most sensitive to DM masses in the range from 30 GeV up to 200–300 GeV. For lighter DM, the signal is reduced, since the available energy to be transferred to the hadronic showers in the tau channel is reduced (we remind that only neutrinos with energy $E_\nu \leq m_\chi$ are produced by the non-relativistic annihilation process). For heavier DM the signal fades away since capture is less efficient and moreover absorption processes of higher energy neutrinos in the Sun start to become operative [26, 27]. These properties can also be observes in figure 5, where the expected number of downward-going ν_τ hadronic events are shown (as solid lines) as a function of the DM mass m_χ, for the same scattering cross section on proton of figure 4, for a detector exposure $M_{\rm det} N_y = 1\,{\rm Mton} \times {\rm year}$. In the same figure, we also show the charged-current events expected from the background ν_τ (horizontal dashed line). This figure demonstrates that the specific ν_τ-induced background is negligible.

4.2 Background events from ν_e and ν_μ neutral-current interactions

As we have already mentioned before, a non-negligible source of background is represented by the atmospheric ν_e and ν_μ neutral current interactions, since a fraction of the Cherenkov ring they produce are misidentified as hadronic tau events. The rate of these events is

JHEP11(2011)133

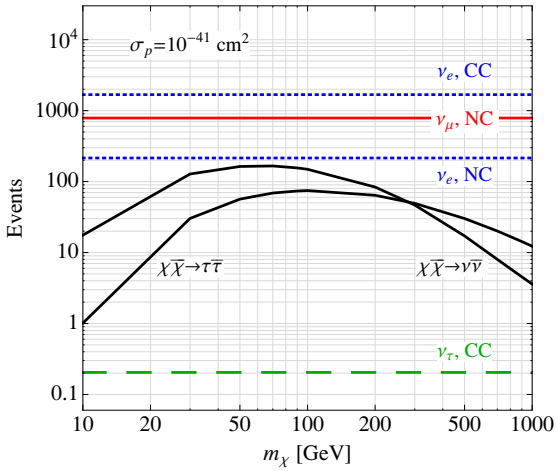

Figure 5. Number of downward-going ν_τ hadronic events (solid lines) as a function of the DM mass m_χ, for a scattering cross section on proton $\sigma = 10^{-41}\,\mathrm{cm}^2$ and for a detector exposure $M_{\rm det}N_y = 1\,\mathrm{Mton}\times\mathrm{year}$. We show also as horizontal lines the neutral current events expected from the atmospheric ν_e (lower dotted blue line) and ν_μ (solid red curve), the charged-current events from ν_e (upper dotted line) and the charged-current events expected from the background ν_τ.

defined as:

$$N^{\mathcal{NC}}_{e,\mu}\big|_{\mathcal{B}} = M_{\rm det}N_y \times \int_{E^{\rm min}_{\rm vis}}^{E^{\rm max}_{\rm vis}} dE_{\rm vis} \int d\Omega\ \eta(\theta)\, \frac{d\mathcal{I}^{\mathcal{NC}}_{e,\mu}}{d\Omega\, dE_{\rm vis}}\bigg|_{\mathcal{B}}\,, \tag{4.8}$$

where $d\mathcal{I}^{\mathcal{NC}}_{e,\mu}/d\Omega\, dE_{\rm vis}$ [50] is:

$$\frac{d\mathcal{I}^{\mathcal{NC}}_{e,\mu}}{d\Omega\, dE_{\rm vis}}\bigg|_{\mathcal{B}} = \int_{E_{\rm vis}}^{\infty} dE_\nu \frac{d\phi_{\nu_e,\nu_\mu}}{d\Omega dE_\nu}\bigg|_{\mathcal{B}} \Sigma^{\mathcal{NC}}_{e,\mu}(E_{\rm vis}, E_\nu) + (\nu \to \bar{\nu})\,. \tag{4.9}$$

The function $\Sigma^{\mathcal{NC}}_{e,\mu}$ is the analogous of eq. (4.3) for neutral current interactions, for which we use the deep-inelastic cross section of ref. [59]. Note that, for neutral current events, the fraction of energy that is transferred to the cascade is given by $y = E_{\rm vis}/E_\nu$, with E_ν being the initial neutrino energy.

The number of neutral current ν_e and ν_μ events for one Mton $\times$ year exposure are reported in figure 5, as horizontal lines. The lower dotted blue line shows the neutral current events expected from the atmospheric ν_e, the solid red curve refers to ν_μ. Together with the charged-current ν_e events (discussed in the next section), these class of events are not directly comparable to the signal events, since they represent a backgound only when they are misidentified as tau hadronic events. Figure 4 shows that these classes of events pose a problem if they are not controlled at a level better than a few percent. This level of misidentification is foreseeable, since SK reconstruction and analysis algorithms are already able to reduce the misidentification at the level of less than 10% [48, 49]. A misidentification level around 1%, together with an efficiency of reconstruction of hadronic tau-events increased of about 70–80% would bring the down-going ν_τ signal to be a competitive search. A possible way to reduce the misidentification background could be obtained by considering specific

JHEP11(2011)133

tau hadronic decays. Indeed, the tau lepton decays mainly producing multiple pion events: about 40% of the hadronic decays are given by $\tau^- \to \pi^0\pi^-\nu_\tau$. This channel produces two electromagnetic cascades from $\pi^0 \to \gamma\gamma$ decay and one muon track from $\pi^- \to \mu^-\bar{\nu}_\mu$ decay. The main experimental challenge would be to find suitable cuts to statistically distinguish these events from the CC/NC ν_e and ν_μ multiple pion productions.

4.3 Background events from ν_e charged-current interactions

Another source of background for the hadronic tau decay is represented by the charged-current ν_e channel. We calculate background events due to ν_e charge current interactions as [50]:

$$N_e^{\mathcal{CC}}\big|_{\mathcal{B}} = M_{\rm det} N_y \times \int_{E_{\rm vis}^{\rm min}}^{E_{\rm vis}^{\rm max}} dE_{\rm vis} \int d\Omega\ \eta(\theta)\, \frac{d\phi_{\nu_e}}{d\Omega dE_{\rm vis}}\bigg|_{\mathcal{B}} \Sigma_{e,\rm TOT}^{\mathcal{CC}}(E_{\rm vis}) + (\nu \to \bar{\nu})\,, \qquad (4.10)$$

where $\Sigma_{e,\rm TOT}^{\mathcal{CC}}$ is the analogous of eq. (4.3) for the total charged-current cross section of ν_e, for which we used the deep-inelastic expressions of ref. [59]. Note that, in this case, the visible energy $E_{\rm vis}$ is equal to the full initial neutrino energy E_ν.

The number of charged current ν_e events for one Mton $\times$ year exposure is reported again in figure 5. We notice that this is the category of events which (through misidentification) represents the largest source of background.

5 Detectability and statistical significance

To quantify the discovery reach of present and future water Cherenkov detectors, we use the statistical significance ς, defined as the signal-to-noise ratio:

$$\varsigma \equiv \frac{S}{\sqrt{S+B}}\,. \qquad (5.1)$$

See also ref. [60] for a complete discussion on the statistical significance. We have studied the behaviour of ς in two cases: an ideal case in which no misidentification is present and the detector efficiency for tau leptons is almost 100%, and a more realistic case in which both the misidentification and the detection efficiency for taus are considered. In the ideal case we have:

$$B_{\rm ideal} = N_\tau^{\mathcal{CC}}\big|_{\mathcal{B}}\,. \qquad (5.2)$$

In the presence of misidentification of the electron $\epsilon_e^{\rm mis}$ and muon $\epsilon_\mu^{\rm mis}$ events and detection efficiency ϵ_τ for the detection of tau hadronic events, we instead have:

$$B_{\rm realistic} = \epsilon_\tau N_\tau^{\mathcal{CC}}\big|_{\mathcal{B}} + \epsilon_\mu^{\rm mis} N_\mu^{\mathcal{NC}}\big|_{\mathcal{B}} + \epsilon_e^{\rm mis}\big(N_e^{\mathcal{NC}}\big|_{\mathcal{B}} + N_e^{\mathcal{CC}}\big|_{\mathcal{B}}\big)\,. \qquad (5.3)$$

Our results are reported in figure 6, 7 and 8. Figure 6 shows the iso-contours of statistical significance for the detection of downward-going ν_τ hadronic events in the plane of detector exposure (in kton $\times$ year) and DM mass m_χ. The left panel refers to DM annihilation into neutrinos, while the right panels stands for annihilation into tau leptons. The elastic scattering cross section on protons (relevant for capture in the Sun) is fixed at

JHEP11(2011)133

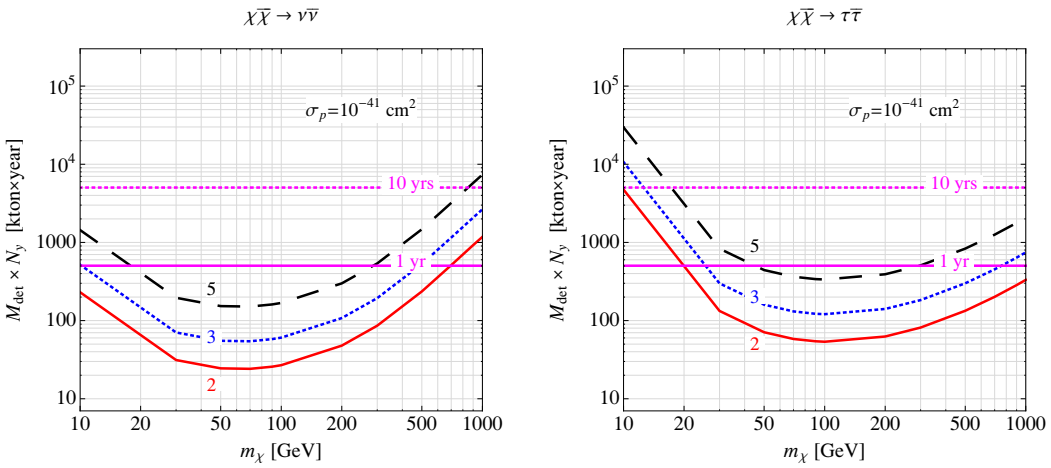

Figure 6. Iso-contours of statistical significance for the detection of downward-going ν_τ hadronic events in the plane of detector exposure (in kton × year) and DM mass m_χ. The left panel refers to DM annihilation into neutrinos, while the right panels stands for annihilation into tau leptons. The elastic scattering cross section on protons (relevant for capture in the Sun) is fixed at the benchmark value of $10^{-41}\,\mathrm{cm}^2$. The solid (red), dotted (blue) and dashed (black) lines refer to significance of 2, 3 and $5\,\sigma$. The two horizontal (pink) lines denote the exposures that can be reached by a 0.5 Mton detector, like HK, in 1 (solid) and 10 (dotted) years. In this plot we assumed full efficiency for the detection of tau hadronic events ($\epsilon_\tau = 100\%$) and no misidentification of electron and muon NC/CC events ($\epsilon_e^{\rm mis} = \epsilon_\mu^{\rm mis} = 0$).

the benchmark value of $10^{-41}\,\mathrm{cm}^2$. The solid (red), dotted (blue) and dashed (black) lines refer to significance of 2, 3 and $5\,\sigma$. The two horizontal (pink) lines denote the exposures that can be reached by a 0.5 Mton detector, like HK, in 1 (solid) and 10 (dotted) years. This plot refers to an ideal detector with full efficiency for the detection of tau hadronic events ($\epsilon_\tau = 100\%$) respect to the neutral and charged current electron and muon events ($\epsilon_e^{\rm mis} = \epsilon_\mu^{\rm mis} = 0$). We notice that in this ideal case a $5\,\sigma$ significance of signal detection is present for a wide DM mass range (from about 20 to 300 GeV) with 1 year of exposure of 1 Mton detector. Indication at the 2–3 σ level are possible up to 500–700 GeV for the case of direct annihilation into neutrinos, while it extends to larger masses (and drops al small DM masses) for the case of annihilation into tau leptons. Clearly, statistical significance scales with the scattering cross section σ_p. Note that a more precise analysis would require to take into account the theoretical uncertainties on the intrinsic ν_τ fluxes [37, 41–43]. The intrinsic contribution constitutes roughly 21% of the total ν_τ events calculated as described in section 4.1. For an intrinsic flux one order of magnitude higher than the one considered here [35], the curves for the statistical significance ς in figure 6 would move up by a factor of 1.3 for the $\tau\bar{\tau}$ annihilation channel and for a DM mass m_χ between 10 and 20 GeV. The curves will remain roughly unchanged for higher masses and for the $\nu\bar{\nu}$ annihilation channel. We will moreover see that in the realistic cases of our interest (with misidentification) the dependence on the intrinsic ν_τ flux is highly reduced.

A more realistic situation requires to take under proper consideration the efficiency for reconstruction of tau events and the misidentification of the ν_e and ν_μ events. This is shown

JHEP11(2011)133

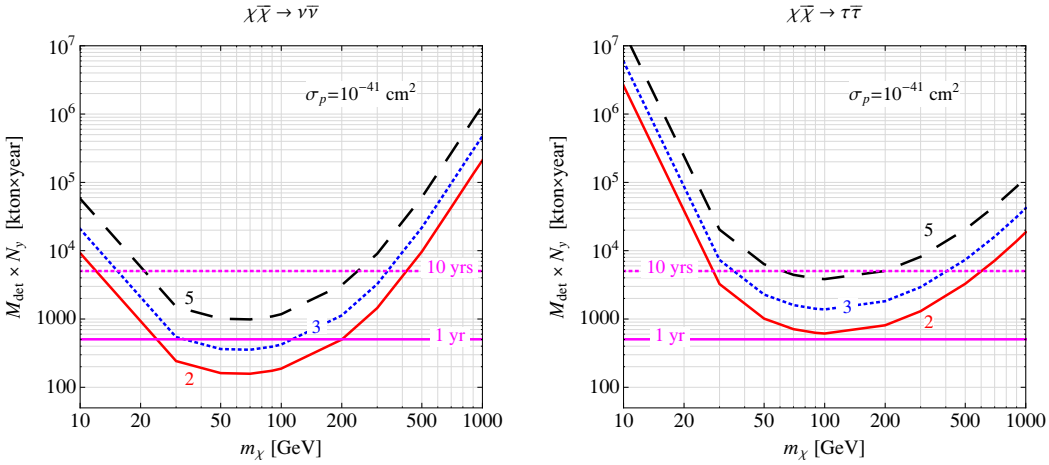

Figure 7. The same as in figure 6, for detection efficiency of tau hadronic events $\epsilon_\tau = 40\%$ and misidentification of electron and muon events $\epsilon_e^{\rm mis} = \epsilon_\mu^{\rm mis} = 4\%$.

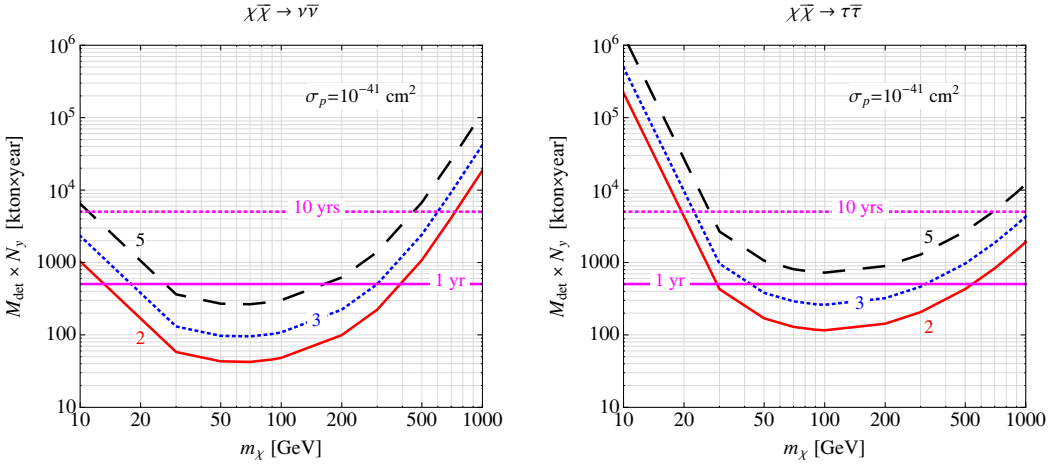

Figure 8. The same as in figure 6, for detection efficiency of tau hadronic events $\epsilon_\tau = 70\%$ and misidentification of electron and muon events $\epsilon_e^{\rm mis} = \epsilon_\mu^{\rm mis} = 1\%$.

in figure 7, where we reduce the efficiency to $\epsilon_\tau = 40\%$ and we allow a misidentification of 4%, both in the electron and muon channels, not far from those already achieved by the SK analysis [48, 49]. We notice that now large statistical significance is recovered with a much larger exposure: nevertheless, a 10 yr period of data taking reproduces the same level of reach as the one discussed for the optimal case in figure 6. Figure 8 shows the capabilities in the case of better performance: $\epsilon_\tau = 70\%$ and $\epsilon_e^{\rm mis} = \epsilon_\mu^{\rm mis} = 1\%$. In this case, a few years of exposure would suffice to cover almost the whole DM mass range (with noticeable differences for different annihilation channels) for our benchmark value of the scattering cross section σ_p. Note that also for $\epsilon_e^{\rm mis} = \epsilon_\mu^{\rm mis} = 1\%$ the background is still dominated by misidentified events, see figure 5, and the uncertainties on the ν_τ intrinsic flux (which account for roughly 21% of the total number of events) does not alter our conclusions.

JHEP11(2011)133

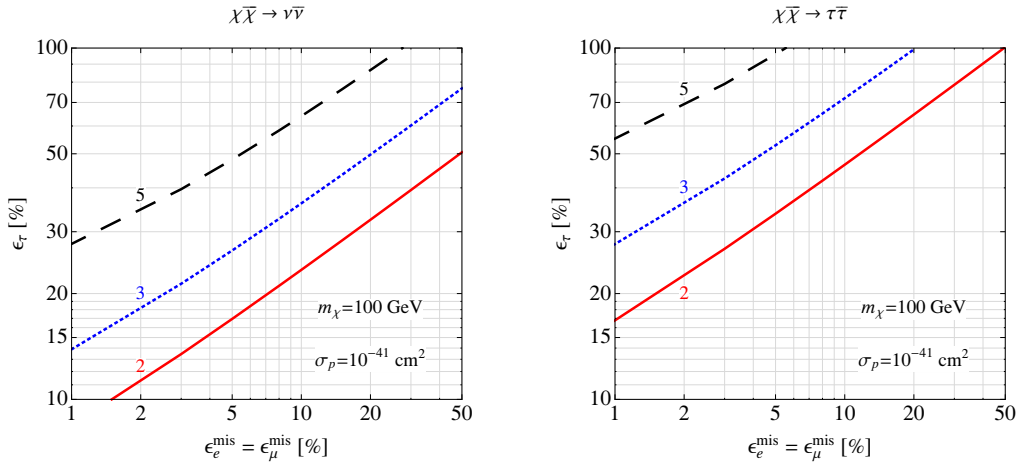

Figure 9. Dependence of the statistical significance ς on the misidentification parameters $\epsilon_e = \epsilon_\mu$ and ϵ_τ, for a DM mass $m_\chi = 100\,\text{GeV}$ with cross section $\sigma_p = 10^{-41}\text{cm}^2$ and an exposure $M_{\rm det}N_y = 1\,\text{Mton} \times \text{year}$. The solid (red), dotted (blue) and dashed (black) lines refer to $\varsigma = 2, 3, 5$. The left panel stands for DM annihilation into neutrinos, while the right panels for annihilation into tau leptons.

The dependence of the statistical significance with the detection efficiencies is reported, as an illustrative example, in figure 9 for a DM mass $m_\chi = 100\,\text{GeV}$ and the benchmark value of σ_p. We notice that an efficiency of tau-events reconstruction of 50–60% would allow to a clear signal detection even without the need to reduce the level of misidentification. At the same time, an alternatively, a reduction of $\epsilon_e^{\rm mis}$ and $\epsilon_\mu^{\rm mis}$ at the 1% level would be enough (for this benchmark case) to obtain a $5\,\sigma$ detection quite easily.

In order to test the sensitivity of the downward-going tau signal not only to the DM mass, but also to its scattering cross section σ_p, we show in figure 10 the contours for $\varsigma = 1.64$ (which corresponds to a C.L. of 90%) in the plane σ_p vs. m_χ, for a detector with exposure $M_{\rm det}N_y = 1\,\text{Mton} \times \text{year}$. The dotted lines represent the limits without considering misidentification, while the solid lines refer to $\epsilon_\tau = 40\%$ and $\epsilon_e^{\rm mis} = \epsilon_\mu^{\rm mis} = 4\%$. The left panel refers to spin independent interactions, while the right panel shows the case for a spin dependent cross section. These curves can alternatively be considered as the 90% C.L. upper bounds deriving from the downward-going hadronic events on σ_p vs. m_χ. In the left panel of figure 10, beside our limits, we show the allowed regions obtained considering the DAMA [61–63], CoGeNT [64] and CRESST [65] positive results. The DAMA and CoGeNT regions are taken from ref. [66] to which we refer for more detailed information. The DAMA region represents the domain where the likelihood function values differ more than $7.5\,\sigma$ from the null hypothesis (absence of modulation), while the CoGeNT region refers to the area where the likelihood function values differ more than $1.64\,\sigma$. We also plot the constraints from XENON [67] and CDMS [68] experiments, as calculated in the statistical analysis of ref. [69]. These limits are taken at $5\,\sigma$ and the XENON threshold has been set to 8 photoelectrons. In the right panel of figure 10, we report the DAMA region in the case of spin-dependent interaction [70]. We also report the limit on spin-

JHEP11(2011)133

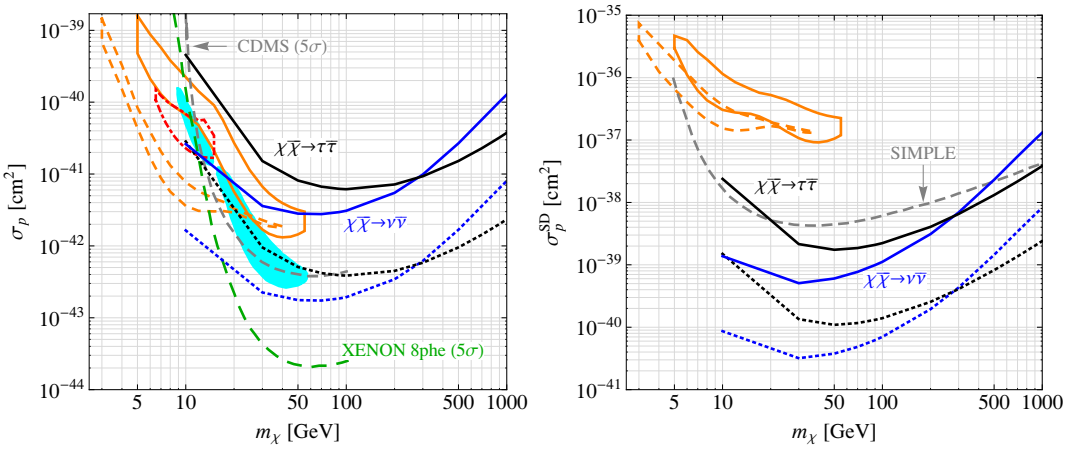

Figure 10. Dependence of the statistical significance ς on the DM scattering cross section on protons σ_p as a function of the DM mass m_χ, that can be derived by using the downward-going hadronic events with an exposure $M_{\rm det}N_y = 1\,{\rm Mton}\times{\rm year}$. The curves refer to $\varsigma = 1.64$ and can alternatively be considered as the 90% C.L. upper bounds deriving from the downward-going hadronic events on σ_p vs. m_χ. The dotted lines represent the limits without considering misidentification, while the solid lines refer to $\epsilon_\tau = 40\%$ and $\epsilon_e^{\rm mis} = \epsilon_\mu^{\rm mis} = 4\%$. *Left panel*: our results for the spin independent case together with the allowed regions from DAMA (orange solid line for the case without channeling, orange dashed line for the channeling case), CoGeNT (dot-dashed red curve) and CRESST (cyan regions), and the limits from XENON 100 (green dashed line) and CDMS (gray dashed line) experiments. *Right panel*: our results for the spin-dependent case, together with the allowed regions from DAMA (upper for no-channeling, lower for channeling) and the limit from SIMPLE (gray dashed line).

dependent interactions from the SIMPLE experiment [71], see also ref. [72] and ref. [73] for discussions on critical points. Further weaker limits, not reported in figure 10, come from the PICASSO [74], COUPP [75] and KIMS [76] experiments. The recent analyses of direct detection annual modulation effects observed by DAMA [61–63] and CoGeNT [64] (and the excess of events reported by CRESST [65]) point toward a light DM candidate with a mass around 10 GeV and spin-independent scattering cross sections of the order of $10^{-42}\,{\rm cm}^2$–$10^{-40}\,{\rm cm}^2$. For this type of particle, we would expect, for the case of direct annihilation into neutrinos, between 9 and 900 hadronic events and a detection with a statistical significance close to $5\,\sigma$ with a 10 years exposure on HK ($5\,{\rm Mton}\times{\rm yr}$) in the case of the improved performance of figure 8.

6 Conclusions

In the context of indirect DM searches with neutrinos, the most common channel of investigation is represented by upward-going muons or by contained μ-like or e-like events produced by the charged-current conversion of the muon- or electron-neutrino fluxes produced by DM annihilation in the Sun or in the Earth. These channels are very solid and do not suffer from large detection difficulties. In the most typical case of upward-going muons, the conversion area for the $\nu_\mu \to \mu$ process is represented by a large portion of the

JHEP11(2011)133

rock below the detector and experimental apparata posses very large detection efficiencies. For instance, SK has almost a 100% efficiency to detect through-going muons. The most important limit for this type of DM searches, instead, is represented by the large ν_μ and ν_e atmospheric background that cast a shadow on the DM signal.

In this paper we propose a new channel for DM searches at neutrino telescopes: downward-going hadronic tau events originated by the ν_τ signal produced by DM annihilation in the Sun. This specific signal potentially represents a very good opportunity for DM, since the background of atmospheric downward-going ν_τ is extremely reduced with respect to the upward-going ν_μ case commonly considered. The intrinsic amount of ν_τ in atmospheric neutrinos is very small as compared to ν_e and ν_μ components, while the ν_τ component in the signal from DM annihilation (or decay) in the Sun is typically expected to be of the same order of their ν_e and ν_μ counterparts. Moreover, in the downward-going direction, atmospheric ν_μ do not have enough baseline to oscillated into ν_τ. Therefore, a flux of tau neutrinos coming from the Sun when the star is above the horizon represents a signal with a very reduced background. The signal-to-background ratio in terms of fluxes is therefore much more favorable for down-going ν_τ's then for up-going ν_μ's and ν_e's (or even ν_τ's themselves).

Additional sources of background are represented by ν_τ produced in the solar corona of the Sun (which represent an irreducible background for our DM signal, since it comes from the same source, the Sun) and in ν_τ arriving at the Earth from the galactic plane, mainly produced by oscillation of ν_μ produced in cosmic-ray interactions with the interstellar medium. This source of background is, in principle, reducible by angular cuts on the galactic plane position. For detectors located in the northern hemisphere the angles $\cos\theta_Z \geq 0.5$ are particularly favourable, because the galactic plane duty-factor is small for those angles. We have shown that all these sources of backgrounds are, by themselves, not posing relevant limits to the DM signal, which therefore represent a potentially viable novel possibility.

The large advantage represented by the reduced background for the downward-going ν_τ fluxes is, unfortunately, partly diminished by limits inherent in the difficulty to detect and properly identify tau neutrinos. Indeed, detectors specifically designed for the identification of tau events, like Opera at Gran Sasso Laboratory, are currently too small to collect a statistically significant number of events. For this reason we have focused our analysis on Cherenkov detectors. In this case the hadronic tau events cannot be easily distinguished by the neutral current events, mostly coming from atmospheric ν_e and ν_μ, and by the charged current e-like events. The possibility to correctly detect hadronic tau events is currently based on statistical methods and the percentage of misidentified events for a SK-like detector is of the order of several percent [48, 49]. As the atmospheric ν_e and ν_μ are more abundant than the signal ν_τ events, the misidentification influences the discovery potential of DM through the downward-going tau channel.

Since for existing Cherenkov detectors, like SK, the number of hadronic tau events expected is small, we have focused our analysis on future Mton-size Cherenkov detectors, like Hyper-Kamiokande [20], UNO [77] or MEMPHYS [78], respectively in Japan, US and France. All these future detectors will be situated in the norther hemisphere and this could

JHEP11(2011)133

represent a great advantage to reduce the background of galactic neutrinos in the study of events from zenith angles $\cos\theta_Z \geq 0.5$. We have not discussed in our analysis the IceCube detector, since ν_τ reconstruction, at the low energies required to study the DM in the mass range of interest in our analysis (10 GeV–1 TeV), may not be possible, but the possibility to implement statistical analyses is under study [79]. For the detection of high energy ν_τ at IceCube see for instance ref. [80].

For the Mton-size water Cherenkov detectors we have shown that the downward-going tau neutrinos signal has potentially good prospects, the main limitation being the level of misidentification of non-tau events, which need to be kept at the level of percent. For definiteness, we have studied two benchmark cases: DM directly annihilating into neutrinos, with equal amount of the three active flavors; dark matter annihilating into tau pairs. We showed that several tens of events per year (depending on the DM mass and annihilation/decay channel) are potentially collectible in a Mton-scale detector. Once the misidentification of non-tau events is taken under consideration, a $5\,\sigma$ significance discovery is potentially reachable for DM masses in the range from 20 to 300 GeV with a few years of exposure, and for a benchmark value of DM scattering cross section on protons (relevant for DM capture in the Sun) of $\sigma_p = 10^{-41}\,\mathrm{cm}^{-2}$. For light DM candidates with a mass around 10 GeV and spin-independent scattering cross sections of the order of $10^{-42}\,\mathrm{cm}^2$–$10^{-40}\,\mathrm{cm}^2$, which are of special current interest due to the recent results in direct detection studies, we find that, for the case of direct annihilation into neutrinos, a detector like HK within 10 years (exposure of $5\,\mathrm{Mton}\times\mathrm{yr}$) could collect between 9 and 900 hadronic tau DM events and be sensitive to detection with a statistical significance close to $5\,\sigma$, in the case of a 70% detection efficiency in the reconstruction of the tau hadronic events and of a 1% level of misidentification of non-tau events.

Acknowledgments

We would like to thank G. Giordano, M.C. Gonzalez-Garcia, O. Mena and I. Mocioiu for useful discussions. We acknowledge Research Grants funded jointly by Ministero dell'Istruzione, dell'Università e della Ricerca (MIUR), by Università di Torino and by Istituto Nazionale di Fisica Nucleare within the *Astroparticle Physics Project* (MIUR contract number: PRIN 2008NR3EBK; INFN grant code: FA51). N.F. acknowledges support of the spanish MICINN Consolider Ingenio 2010 Programme under grant MULTIDARK CSD2009-00064. This work was partly completed at the Theory Division of CERN in the context of the TH-Institute 'Dark Matter Underground and in the Heavens' (DMUH11, 18–29 July 2011).

References

[1] T.K. Gaisser, G. Steigman and S. Tilav, *Limits on cold dark matter candidates from deep underground detectors*, *Phys. Rev.* **D 34** (1986) 2206 [INSPIRE].

[2] J. Silk, K.A. Olive and M. Srednicki, *The photino, the Sun and high-energy neutrinos*, *Phys. Rev. Lett.* **55** (1985) 257 [INSPIRE].

JHEP11(2011)133

[3] K. Freese, *Can scalar neutrinos or massive Dirac neutrinos be the missing mass?*, *Phys. Lett.* **B 167** (1986) 295 [INSPIRE].

[4] L.M. Krauss, K. Freese, W. Press and D. Spergel, *Cold dark matter candidates and the solar neutrino problem*, *Astrophys. J.* **299** (1985) 1001 [INSPIRE].

[5] L.M. Krauss, M. Srednicki and F. Wilczek, *Solar system constraints and signatures for dark matter candidates*, *Phys. Rev.* **D 33** (1986) 2079, revised version of preprint NSF-ITP-85-58 [INSPIRE].

[6] L. Bergstrom, J. Edsjo and P. Gondolo, *Indirect neutralino detection rates in neutrino telescopes*, *Phys. Rev.* **D 55** (1997) 1765 [hep-ph/9607237] [INSPIRE].

[7] A. Bottino, V. de Alfaro, N. Fornengo, G. Mignola and M. Pignone, *Indirect search for neutralinos at neutrino telescopes*, *Phys. Lett.* **B 265** (1991) 57 [INSPIRE].

[8] A. Bottino, N. Fornengo, G. Mignola and L. Moscoso, *Signals of neutralino dark matter from Earth and Sun*, *Astropart. Phys.* **3** (1995) 65 [hep-ph/9408391] [INSPIRE].

[9] A. Bottino, F. Donato, N. Fornengo and S. Scopel, *Indirect signals from light neutralinos in supersymmetric models without gaugino mass unification*, *Phys. Rev.* **D 70** (2004) 015005 [hep-ph/0401186] [INSPIRE].

[10] Super-Kamiokande collaboration, S. Desai et al., *Search for dark matter WIMPs using upward through-going muons in Super-Kamiokande*, *Phys. Rev.* **D 70** (2004) 083523 [*Erratum ibid.* **D 70** (2004) 109901] [hep-ex/0404025] [INSPIRE].

[11] AMANDA collaboration, M. Ackermann et al., *Limits to the muon flux from neutralino annihilations in the Sun with the AMANDA detector*, *Astropart. Phys.* **24** (2006) 459 [astro-ph/0508518] [INSPIRE].

[12] IceCube collaboration, R. Abbasi et al., *Limits on a muon flux from neutralino annihilations in the Sun with the IceCube 22-string detector*, *Phys. Rev. Lett.* **102** (2009) 201302 [arXiv:0902.2460] [INSPIRE].

[13] V. Niro, A. Bottino, N. Fornengo and S. Scopel, *Investigating light neutralinos at neutrino telescopes*, *Phys. Rev.* **D 80** (2009) 095019 [arXiv:0909.2348] [INSPIRE].

[14] R. Kappl and M.W. Winkler, *New limits on dark matter from Super-Kamiokande*, *Nucl. Phys.* **B 850** (2011) 505 [arXiv:1104.0679] [INSPIRE].

[15] F.-F. Lee and G.-L. Lin, *Probing annihilations and decays of low-mass galactic dark matter in IceCube DeepCore array — Part I: track events*, arXiv:1105.5719 [INSPIRE].

[16] S.K. Agarwalla, M. Blennow, E.F. Martinez and O. Mena, *Neutrino probes of the nature of light dark matter*, *JCAP* **09** (2011) 004 [arXiv:1105.4077] [INSPIRE].

[17] O. Mena, S. Palomares-Ruiz and S. Pascoli, *Reconstructing WIMP properties with neutrino detectors*, *Phys. Lett.* **B 664** (2008) 92 [arXiv:0706.3909] [INSPIRE].

[18] J. Kumar, J.G. Learned, M. Sakai and S. Smith, *Dark matter detection with electron neutrinos in liquid scintillation detectors*, *Phys. Rev.* **D 84** (2011) 036007 [arXiv:1103.3270] [INSPIRE].

[19] M. Honda, T. Kajita, K. Kasahara and S. Midorikawa, *A new calculation of the atmospheric neutrino flux in a 3-dimensional scheme*, *Phys. Rev.* **D 70** (2004) 043008 [astro-ph/0404457] [INSPIRE].

[20] K. Nakamura, *Hyper-Kamiokande: a next generation water Cherenkov detector*, *Int. J. Mod. Phys.* **A 18** (2003) 4053 [INSPIRE].

JHEP11(2011)133

[21] L. Covi, M. Grefe, A. Ibarra and D. Tran, *Unstable gravitino dark matter and neutrino flux*, *JCAP* **01** (2009) 029 [arXiv:0809.5030] [INSPIRE].

[22] J. Jones, I. Mocioiu, I. Sarcevic and M. Reno, *Tracing very high energy tau neutrinos from cosmological sources in ice*, *Int. J. Mod. Phys.* **A 20** (2005) 1204 [hep-ph/0408060] [INSPIRE].

[23] S.I. Dutta, M.H. Reno and I. Sarcevic, *Tau neutrinos underground: signals of muon-neutrino → tau neutrino oscillations with extragalactic neutrinos*, *Phys. Rev.* **D 62** (2000) 123001 [hep-ph/0005310] [INSPIRE].

[24] J. Conrad, A. de Gouvêa, S. Shalgar and J. Spitz, *Atmospheric tau neutrinos in a multi-kiloton liquid argon detector*, *Phys. Rev.* **D 82** (2010) 093012 [arXiv:1008.2984] [INSPIRE].

[25] T. Stanev, *Possible tau appearance experiment with atmospheric neutrinos*, *Phys. Rev. Lett.* **83** (1999) 5427 [astro-ph/9907018] [INSPIRE].

[26] M. Cirelli et al., *Spectra of neutrinos from dark matter annihilations*, *Nucl. Phys.* **B 727** (2005) 99 [*Erratum ibid.* **B 790** (2008) 338-344] [hep-ph/0506298] [INSPIRE].

[27] M. Blennow, J. Edsjo and T. Ohlsson, *Neutrinos from WIMP annihilations using a full three-flavor Monte Carlo*, *JCAP* **01** (2008) 021 [arXiv:0709.3898] [INSPIRE].

[28] T. Schwetz, M. Tórtola and J.W.F. Valle, *Global neutrino data and recent reactor fluxes: status of three-flavour oscillation parameters*, *New J. Phys.* **13** (2011) 063004 [arXiv:1103.0734] [INSPIRE].

[29] A. Gould, *Resonant enhancements in WIMP capture by the Earth*, *Astrophys. J.* **321** (1987) 571 [INSPIRE].

[30] A. Gould, *Direct and indirect capture of WIMPs by the Earth*, *Astrophys. J.* **328** (1988) 919 [INSPIRE].

[31] A. Gould, *Gravitational diffusion of solar system WIMPs*, *Astrophys. J.* **368** (1991) 610.

[32] O. Probst, *The apparent motion of the Sun revisited*, *Eur. J. Phys.* **23** (2002) 315.

[33] M. Honda, T. Kajita, K. Kasahara and S. Midorikawa, *Improvement of low energy atmospheric neutrino flux calculation using the JAM nuclear interaction model*, *Phys. Rev.* **D 83** (2011) 123001 [arXiv:1102.2688] [INSPIRE].

[34] K. Niita et al., *PHITS — a particle and heavy ion transport code system*, *Radiat. Meas.* **41** (2006) 1080 [INSPIRE].

[35] L. Pasquali and M. Reno, *Tau-neutrino fluxes from atmospheric charm*, *Phys. Rev.* **D 59** (1999) 093003 [hep-ph/9811268] [INSPIRE].

[36] F.-F. Lee and G.-L. Lin, *A semi-analytic calculation on the atmospheric tau neutrino flux in the GeV to TeV range*, *Astropart. Phys.* **25** (2006) 64 [hep-ph/0412383] [INSPIRE].

[37] C. Costa, *The prompt lepton cookbook*, *Astropart. Phys.* **16** (2001) 193 [hep-ph/0010306] [INSPIRE].

[38] A. Kaidalov and O. Piskunova, *Inclusive spectra of baryons in the quark-gluon strings model*, *Z. Phys.* **C 30** (1986) 145 [INSPIRE].

[39] E. Bugaev et al., *Atmospheric muon flux at sea level, underground and underwater*, *Phys. Rev.* **D 58** (1998) 054001 [hep-ph/9803488] [INSPIRE].

JHEP11(2011)133

[40] P. Gondolo, G. Ingelman and M. Thunman, *Charm production and high-energy atmospheric muon and neutrino fluxes*, *Astropart. Phys.* **5** (1996) 309 [hep-ph/9505417] [INSPIRE].

[41] C. Costa, F. Halzen and C. Salles, *The prompt TeV–PeV atmospheric neutrino window*, *Phys. Rev.* **D 66** (2002) 113002 [hep-ph/0104039] [INSPIRE].

[42] C. Costa and C. Salles, *Prompt atmospheric neutrinos: phenomenology and implications*, hep-ph/0105271 [INSPIRE].

[43] R. Enberg, M.H. Reno and I. Sarcevic, *Prompt neutrino fluxes from atmospheric charm*, *Phys. Rev.* **D 78** (2008) 043005 [arXiv:0806.0418] [INSPIRE].

[44] G. Ingelman and M. Thunman, *High-energy neutrino production by cosmic ray interactions in the Sun*, *Phys. Rev.* **D 54** (1996) 4385 [hep-ph/9604288] [INSPIRE].

[45] H. Athar and C. Kim, *Gev to TeV astrophysical tau neutrinos*, *Phys. Lett.* **B 598** (2004) 1 [hep-ph/0407182] [INSPIRE].

[46] H. Athar, F.-F. Lee and G.-L. Lin, *Tau neutrino astronomy in GeV energies*, *Phys. Rev.* **D 71** (2005) 103008 [hep-ph/0407183] [INSPIRE].

[47] T. DeYoung, S. Razzaque and D. Cowen, *Astrophysical tau neutrino detection in kilometer-scale Cherenkov detectors via muonic tau decay*, *Astropart. Phys.* **27** (2007) 238 [astro-ph/0608486] [INSPIRE].

[48] SUPER-KAMIOKANDE collaboration, K. Abe et al., *A measurement of atmospheric neutrino flux consistent with tau neutrino appearance*, *Phys. Rev. Lett.* **97** (2006) 171801 [hep-ex/0607059] [INSPIRE].

[49] T. Kato, *Tau neutrino appearance via neutrino oscillations in atmospheric neutrinos*, Ph.D. Thesis, Stony Brook University, New York U.S.A. (2007).

[50] G. Giordano, O. Mena and I. Mocioiu, *Atmospheric neutrino oscillations and tau neutrinos in ice*, *Phys. Rev.* **D 81** (2010) 113008 [arXiv:1004.3519] [INSPIRE].

[51] H. Nunokawa, O. Peres and R. Zukanovich Funchal, *Probing the LSND mass scale and four neutrino scenarios with a neutrino telescope*, *Phys. Lett.* **B 562** (2003) 279 [hep-ph/0302039] [INSPIRE].

[52] Y.S. Jeong and M.H. Reno, *Tau neutrino and antineutrino cross sections*, *Phys. Rev.* **D 82** (2010) 033010 [arXiv:1007.1966] [INSPIRE].

[53] S. Kretzer and M. Reno, *Tau neutrino deep inelastic charged current interactions*, *Phys. Rev.* **D 66** (2002) 113007 [hep-ph/0208187] [INSPIRE].

[54] A. Martin, W. Stirling, R. Thorne and G. Watt, *Parton distributions for the LHC*, *Eur. Phys. J.* **C 63** (2009) 189 [arXiv:0901.0002] [INSPIRE].

[55] http://durpdg.dur.ac.uk/HEPDATA/PDF.

[56] M. Reno, *Electromagnetic structure functions and neutrino nucleon scattering*, *Phys. Rev.* **D 74** (2006) 033001 [hep-ph/0605295] [INSPIRE].

[57] S. Kretzer and M. Reno, *Target mass corrections to electroweak structure functions and perturbative neutrino cross-sections*, *Phys. Rev.* **D 69** (2004) 034002 [hep-ph/0307023] [INSPIRE].

[58] P. Lipari, *Lepton spectra in the Earth's atmosphere*, *Astropart. Phys.* **1** (1993) 195 [INSPIRE].

[59] A. Strumia and F. Vissani, *Neutrino masses and mixings and...*, hep-ph/0606054 [INSPIRE].

[60] Y.-S. Zhu, *On statistical significance of signal*, *High Energy Phys. Nucl. Phys.* **30** (2006) 331 [arXiv:0812.2708] [INSPIRE].

JHEP11(2011)133

[61] R. Bernabei et al., *Searching for WIMPs by the annual modulation signature*, *Phys. Lett.* **B 424** (1998) 195 [INSPIRE].

[62] DAMA collaboration, R. Bernabei et al., *First results from DAMA/LIBRA and the combined results with DAMA/NaI*, *Eur. Phys. J.* **C 56** (2008) 333 [arXiv:0804.2741] [INSPIRE].

[63] R. Bernabei et al., *New results from DAMA/LIBRA*, *Eur. Phys. J.* **C 67** (2010) 39 [arXiv:1002.1028] [INSPIRE].

[64] C. Aalseth et al., *Search for an annual modulation in a P-type point contact germanium dark matter detector*, *Phys. Rev. Lett.* **107** (2011) 141301 [arXiv:1106.0650] [INSPIRE].

[65] G. Angloher et al., *Results from 730 kg days of the CRESST-II dark matter search*, arXiv:1109.0702 [INSPIRE].

[66] P. Belli et al., *Observations of annual modulation in direct detection of relic particles and light neutralinos*, *Phys. Rev.* **D 84** (2011) 055014 [arXiv:1106.4667] [INSPIRE].

[67] XENON100 collaboration, E. Aprile et al., *Dark matter results from 100 live days of XENON100 data*, *Phys. Rev. Lett.* **107** (2011) 131302 [arXiv:1104.2549] [INSPIRE].

[68] The CDMS-II collaboration, Z. Ahmed et al., *Dark matter search results from the CDMS II experiment*, *Science* **327** (2010) 1619 [arXiv:0912.3592] [INSPIRE].

[69] N. Fornengo, P. Panci and M. Regis, *Long-range forces in direct dark matter searches*, arXiv:1108.4661 [INSPIRE].

[70] DAMA collaboration, private communication.

[71] M. Felizardo et al., *Final analysis and results of the phase II SIMPLE dark matter search*, arXiv:1106.3014 [INSPIRE].

[72] J.I. Collar, *Comments on 'Final analysis and results of the phase II SIMPLE dark matter search'*, arXiv:1106.3559 [INSPIRE].

[73] The SIMPLE collaboration, *Reply to arXiv:1106.3559 by J.I. Collar*, arXiv:1107.1515 [INSPIRE].

[74] S. Archambault et al., *Dark matter spin-dependent limits for WIMP interactions on F-19 by PICASSO*, *Phys. Lett.* **B 682** (2009) 185 [arXiv:0907.0307] [INSPIRE].

[75] E. Behnke et al., *Improved limits on spin-dependent WIMP-proton interactions from a two liter CF_3I bubble chamber*, *Phys. Rev. Lett.* **106** (2011) 021303 [arXiv:1008.3518] [INSPIRE].

[76] KIMS collaboration, H. Lee et al., *Limits on WIMP-nucleon cross section with CsI(Tl) crystal detectors*, *Phys. Rev. Lett.* **99** (2007) 091301 [arXiv:0704.0423] [INSPIRE].

[77] C.K. Jung, *Feasibility of a next generation underground water Cherenkov detector: UNO*, *AIP Conf. Proc.* **533** (2000) 29 [hep-ex/0005046] [INSPIRE].

[78] A. de Bellefon et al., *MEMPHYS: a large scale water Cerenkov detector at Frejus*, hep-ex/0607026 [INSPIRE].

[79] D. Grant, D.J. Koskinen and C. Rott, *Fundamental neutrino measurements with IceCube DeepCore*, in Proceedings of the *31st International Cosmic Ray Conference*, University of Łódź, Poland, July 7–15, 2009.

[80] S.-H. Seo, *IceCube: neutrino telescope at the South Pole*, in Proceedings of the *21st Les Rencontres de Physique de la Vallee d'Aoste — Results and Perspectives in Particle Physics*, La Thuile, Aosta Italy, March 4–10, 2007.

JHEP11(2011)133